

Stephen F. Austin State University

SFA ScholarWorks

---

Faculty Publications

Chemistry and Biochemistry

---

2003

## Dendritic Surfactants Show Evidence for Frustrated Intercalation: A New Organoclay Morphology

Erick J. Acosta

*Texas A & M University - College Station*

Youjun Deng

*Texas A & M University - College Station*

G. Norman White

*Texas A & M University - College Station*

Joe B. Dixon

*Texas A & M University - College Station*

Kevin J. McInnes

*Texas A & M University - College Station*

*See next page for additional authors*

Follow this and additional works at: [https://scholarworks.sfasu.edu/chemistry\\_facultypubs](https://scholarworks.sfasu.edu/chemistry_facultypubs)

 Part of the [Chemistry Commons](#)

[Tell us](#) how this article helped you.

---

### Repository Citation

Acosta, Erick J.; Deng, Youjun; White, G. Norman; Dixon, Joe B.; McInnes, Kevin J.; Senseman, Scott A.; Frantzen, Alyx S.; and Simanek, Eric E., "Dendritic Surfactants Show Evidence for Frustrated Intercalation: A New Organoclay Morphology" (2003). *Faculty Publications*. 33.

[https://scholarworks.sfasu.edu/chemistry\\_facultypubs/33](https://scholarworks.sfasu.edu/chemistry_facultypubs/33)

This Article is brought to you for free and open access by the Chemistry and Biochemistry at SFA ScholarWorks. It has been accepted for inclusion in Faculty Publications by an authorized administrator of SFA ScholarWorks. For more information, please contact [cdsscholarworks@sfasu.edu](mailto:cdsscholarworks@sfasu.edu).

---

**Authors**

Erick J. Acosta, Youjun Deng, G. Norman White, Joe B. Dixon, Kevin J. McInnes, Scott A. Senseman, Alyx S. Frantzen, and Eric E. Simanek

# Dendritic Surfactants Show Evidence for Frustrated Intercalation: A New Organoclay Morphology

Erick J. Acosta,<sup>†</sup> Youjun Deng,<sup>†</sup> G. Norman White,<sup>†</sup> Joe B. Dixon,<sup>†</sup>  
Kevin J. McInnes,<sup>†</sup> Scott A. Senseman,<sup>†</sup> Alyx S. Frantzen,<sup>‡</sup> and  
Eric E. Simanek<sup>\*,†</sup>

Departments of Chemistry and Soil and Crop Sciences, Texas A&M University,  
College Station, Texas 77843-3255, and Department of Chemistry,  
Stephen F. Austin State University, Nacogdoches, Texas 75962

Received February 19, 2003. Revised Manuscript Received May 9, 2003

Mixing a smectite clay with some dendritic surfactants shows that despite the large size of some of these molecules, a property that frustrates complete intercalation into the gallery of the clay, organoclay materials are obtained. X-ray powder diffraction (XPD) reveals no significant increases in lattice spacing as these surfactants are added. Infrared (IR) spectroscopy and thermal gravimetric analysis (TGA) show that interlayer water is preserved. Consistent with an undisturbed interlayer, the amount of organic material in organoclays derived from frustrated surfactants does not exceed 15% of the cationic exchange capacity (CEC) of the composite. Smaller dendritic surfactants do not display frustrated intercalation and instead readily enter into the gallery of the smectic clay yielding traditional organoclay materials. A range of organic compositions (5–50% w/w) that exceed the CEC of the materials are observed. The organic content is corroborated by UV spectroscopy and TGA. XPD reveals increasing lattice spacings with increasing organic content. IR spectroscopy and TGA support an increasingly hydrophobic interlayer. A linear isomer of a frustrated surfactant can intercalate into the gallery (5–33% w/w) yielding morphologies that depend on the amount of surfactant added. These results support the hypothesis that shape, and not only size, is important for producing frustrated intercalation.

## Introduction

The structure of the organic component has a profound effect on the morphology of the resulting organoclay material. Ordered monolayers and bilayers have been observed in organoclays derived from aliphatic alcohols and amines.<sup>1</sup> Polymers show evidence for serpentine intercalation of the linear polymer chain, leading to extended or coiled structures that transit the interlayer.<sup>2,3</sup> Formation of these organoclay composites is facilitated through attractive interactions between the clay (or its absorbed cations) and the organic additive. The paradigm for interactions between small molecules and clay is the exchange of alkylammonium ions with absorbed cations. The higher-order morphologies obtained, monolayers and bilayers, are the result of additional stabilizing van der Waals interactions between these linear alkanes. Similar structures with other polar functional groups (i.e., alcohols) are also obtained, although the anchoring interaction with the clay presumably is mediated through the cation or available water molecules. Polymer–clay interactions depend on the nature of the polymer. Polar, linear

polymers including poly(ethylene oxide)<sup>4,5</sup> or nylon<sup>6</sup> can provide polar groups to interact with the cation. To incorporate hydrophobic polymers based on styrene and its derivatives<sup>7,8</sup> or poly(dimethylsiloxane)<sup>9</sup> into the gallery of the clays, the clays are treated first with a hydrophobic surfactant to facilitate interactions with the clay through the surfactant molecule. These surfactants can play an additional role, that of a curing agent.<sup>10</sup>

Branched surfactants including dendrimers<sup>11–13</sup> (or constituents thereof) offer an interesting energetic challenge to the formation of organoclay composites. A dendritic surfactant bearing a cationic anchor could favorably participate in cation exchange, but the inability of dendrimers to pack together in ordered arrays

(4) Ruiz-Hitzky, E.; Aranda, P.; Casal, B.; Galvan, J. C. *Adv. Mater.* **1995**, *7*, 180–184.

(5) Hernan, L.; Morales, J.; Santos, J. *J. Solid State Chem.* **1998**, *141*, 323–329.

(6) Okada, A.; Usuki, A. *Mater. Sci. Eng.* **1995**, *C3*, 109.

(7) Vaia, R. A.; Jandt, K. D.; Kramer, E. J.; Giannelis, E. P. *Chem. Mater.* **1996**, *8*, 2628–2635.

(8) Vaia, R. A.; Ishii, H.; Giannelis, E. P. *Chem. Mater.* **1993**, *5*, 1694–1696.

(9) Burnside, S. D.; Giannelis, E. P. *Chem. Mater.* **1995**, *7*, 1597–1600.

(10) Traintafillidis, C. S.; LeBaron, P. C.; Pinnavaia, T. J. *Chem. Mater.* **2002**, *14*, 4088–4095.

(11) Newkome, G. R.; He, E.; Moorefield, C. N. *Chem. Rev.* **1999**, *99*, 1689–1746.

(12) Bosman, A. W.; Janssen, H. M.; Meijer, E. W. *Chem. Rev.* **1999**, *99*, 1665–1688.

(13) Vögtle, F.; Fischer, M. *Angew. Chem., Int. Ed. Engl.* **1999**, *38*, 4000–4021.

<sup>†</sup> Texas A&M University.

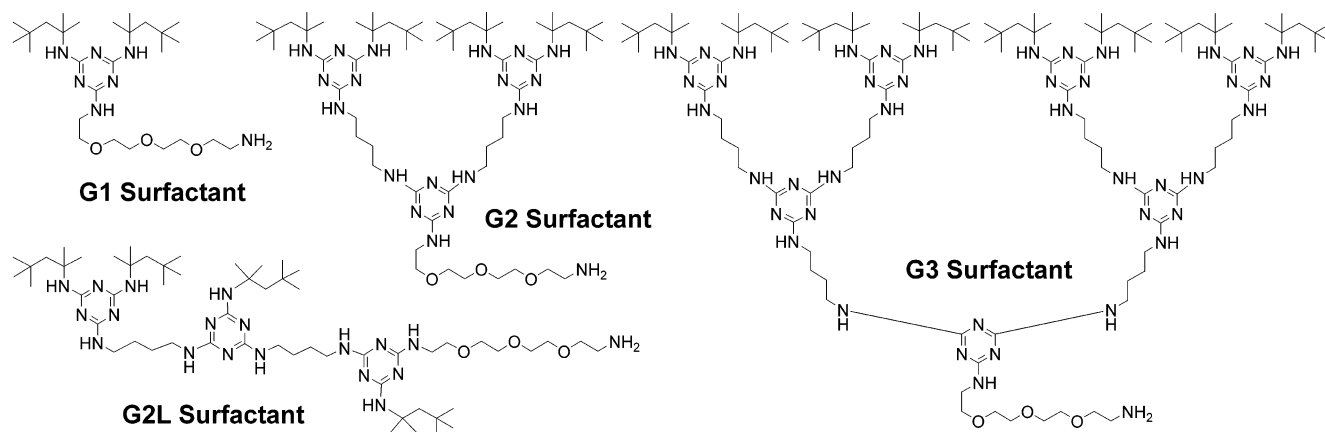
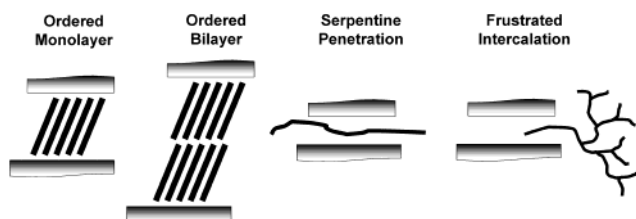
<sup>‡</sup> Stephen F. Austin State University.

(1) Theng, B. K. G. *The Chemistry of Clay–Organic Reactions*; John Wiley and Sons: New York, 1974.

(2) Pinnavaia, T. J.; Beall, G. W., Eds. *Polymer–Clay Nanocomposites*; John Wiley & Sons Ltd.: New York, 2000.

(3) Lagaly, G. In *Developments in Ionic Polymers*; Wilson, A. D., Prosser, H. J., Eds.; Elsevier: London, 1986; pp 77–140.

Chart 1

Scheme 1. Morphologies of Organoclay Composites<sup>a</sup>

<sup>a</sup> We hypothesize the existence of a novel morphology described as frustrated intercalation (characterized by reduced organic content, a relatively hydrophilic interlayer, and a small interlayer lattice spacing) wherein the branched portion precludes complete intercalation.

without severe entropic penalties should preclude stabilizing interactions derived from monolayer or bilayer formation. The cationic group may not offer a significant driving force for interaction with the clay at all. Instead, these materials could separate into two phases. Alternatively, an energetic compromise could be reached wherein the cationic group anchors the dendron to the clay surface and the gallery of the clay is left unmodified. We describe such a morphology as *frustrated intercalation* (Scheme 1). This morphology should be characterized by (i) a reduced organic content in the organoclay in comparison to small-molecule surfactants, (ii) a reasonably hydrophilic interlayer, and (iii) a small interlayer lattice spacing.

Dendrimer–clay interactions have attracted only limited experimental and computational attention. Månson and co-workers mixed three generations of dendrimers based on bis(hydroxymethyl)propanoic acid (BHP; Perstorp, Sweden) with sodium montmorillonite and found that exfoliation predominates.<sup>14</sup> This dendrimer offers no opportunity for cation-exchange reactions with clay but displays multiple hydroxyl groups available for polar interactions. Singh and Balazs have modeled the interaction of star polymers with clays.<sup>15</sup> When the interaction between the star and clay is favorable, linear polymers show a local minimum corresponding to an idealized structure while multi-armed (globular) polymers show a global minimum favoring infinite interlayer spacings (ILSs; exfoliation), a finding

similar to Månson's experimental result. When the interaction between the clay and star is unfavorable, the opposite trend holds: the multi-armed star shows an intercalated structure.

This study describes the exploration of four dendritic surfactants based on triazines interconnected with diamines (Chart 1).<sup>16–19</sup> These surfactants differ in size from generation one, **G1**, to generation three, **G3**, with molecular weights ranging from 526 to 2282 g/mol. Two second-generation surfactants, a dendritic **G2** and a linear **G2L**, are isomers with identical molecular weights (1112 g/mol) to allow us to evaluate size and shape effects. These molecules are slightly different than those reported by Månson or Balazs in that they are neither star polymers nor dendrimers. Additionally, these molecules presumably interact with the clay differently. That is, the surfactants described here can participate in a single cationic exchange reaction while the BHP dendrimers are limited to the potential for multivalent (although individually weaker) interactions between the polar hydroxyl groups and the clay surface.

## Experimental Section

**Clay Preparation.** The smectite clay is a bentonite powder obtained from Southern Clay Products, Gonzalez, TX (CEC = 81.2 mequiv/100 g of clay). The clay is treated with dithionite–citrate–bicarbonate to remove iron oxides, with hydrogen peroxide to eliminate residual organic material, and then with sodium acetate to remove the carbonate minerals. Procedure: 25 g of clay powder is transferred to a 250 mL Nalgene centrifuge tube and mixed with 100 mL of a 1 M pH 5 sodium acetate solution. The mixtures are heated to 90 °C in a water bath and occasionally stirred. After 1 h, the sample is centrifuged at 2000 rpm for 5 min and the supernatant is decanted. This treatment is repeated twice to make sure the sample is free from carbonate minerals. The sediment in the centrifuge tube is washed once with 1 M sodium chloride and subsequently washed several times with a solution of 0.15 g/L of pH 10 sodium carbonate to remove the excess sodium acetate. Then, the sample is passed through a 325 mesh sieve to separate the sand fraction (>50 μm). The remaining clay and silt mixture is transferred to a 250 mL centrifuge tube and the height of the suspension adjusted to 10 cm with the

(16) Zhang, W.; Simanek, E. E. *Org. Lett.* **2000**, 843–845.

(17) Zhang, W.; Simanek, E. E. *Tetrahedron Lett.* **2001**, 42, 5355–5357.

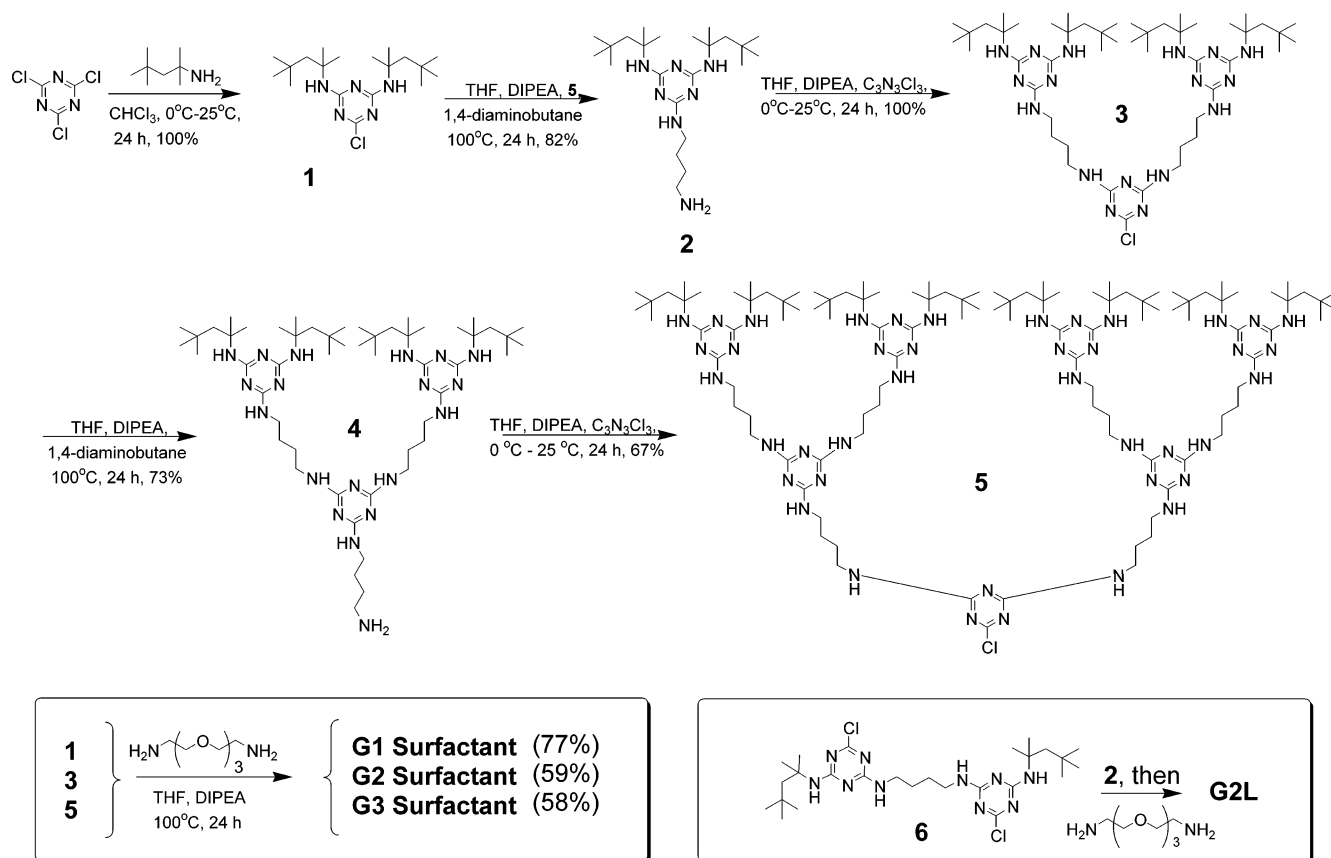
(18) Zhang, W.; Nowlan, D. T., III; Thomson, L. M.; Lackowski, W. M.; Simanek, E. E. *J. Am. Chem. Soc.* **2001**, 123, 8914–8922.

(19) Zhang, W.; Gonzalez, S. O.; Simanek, E. E. *Macromolecules* **2002**, 35, 9015–9021.

(14) Plummer, C. J. G.; Garamszegi, L.; Letierrier, Y.; Rodlert, M.; Månson, J.-A. E. *Chem. Mater.* **2002**, 14, 486–488.

(15) Singh, C.; Balazs, A. C. *Polym. Int.* **2000**, 49, 469–471.

## Scheme 2. Synthesis of the Surfactants



pH 10 sodium carbonate solution. Clay (<2  $\mu\text{m}$ ) and silt (2–50  $\mu\text{m}$ ) fractions are separated by centrifuge at 750 rpm for 3.2 min. The silts are deposited at the bottom of the centrifuge tube, and the clay fraction remained suspended in the solution. The suspension is collected in a 4 L plastic beaker. The separation by centrifugation is repeated until the supernatant becomes clear. The clay suspension is flocculated with a solution of 0.5 M calcium chloride. The flocculated suspension is dialyzed to remove the excess of salt. The clay is freeze-dried, ground, and passed through a 140 mesh sieve.

**Organoclay Preparation.** A series of organoclay composites containing different weight percents of dendritic surfactant were prepared for each dendrimer generation. First, clay suspensions were prepared by adding 20 mL of distilled water to 500 mg of  $\text{Ca}^{2+}$ -saturated clay. To these suspensions was added dropwise 5 mL of a surfactant solution. For the **G1** dendrimer–clay materials, solutions containing 25, 50, 100, 150, 200, 250, and 500 mg of the dendrimer in acetone were used to prepare seven different formulations. For the **G2**, **G2L**, and **G3** dendrimer–clay materials, six formulations of each were prepared by adding 25, 50, 100, 150, 200, and 250 mg of the dendrimers dissolved in tetrahydrofuran (THF) to the clay suspensions. Both organic solvents are completely miscible with water. The organoclay suspensions are incubated, while shaking, for at least 16 h. The organoclay composite is separated by centrifugation and rinsed with water twice to remove any excess of surfactant. The solid materials are vacuum-dried and ground for IR or XPD analysis.

**Dendritic Surfactants.** The three generations (**G1**–**G3**) of dendritic surfactants explored compromise hydrophobic *tert*-octyl groups, triazine rings, and a primary amine to anchor the surfactant to the clay. Scheme 2 shows the synthesis of the melamine-based dendritic surfactants using the convergent method. Surfactant **G1** is prepared in two steps in 76% overall yield. Surfactants **G2** and **G3** are available in four and six steps in 47% and 23% overall yield, respectively. The linear analogue of **G2**, **G2L**, is prepared in four steps in 30% overall yield. Synthesis and characterization data for **G1**, **G2**, **G2L**, **G3**, and **1**–**6** are described in the following paragraphs.

**G1 Surfactant.** Intermediate **1** (1.0 g, 2.7 mmol) is dissolved in 30 mL of chloroform, and diisopropylethylamine (DIPEA; 1.0 mL, 5.7 mmol) is added to the solution. Jeffamine EDR-192 (1.6 g, 8.3 mmol) is added, and the solution is stirred at 100°C for 24 h. The crude product is concentrated and purified by silica gel chromatography using 9:1  $\text{CH}_2\text{Cl}_2/\text{CH}_3\text{OH}$  to give a pale yellow oil (0.90 g, 1.7 mmol) in 63% yield:  $^1\text{H NMR}$  (300 MHz,  $\text{CDCl}_3$ )  $\delta$  3.63 (m, 16 H), 2.93 (t, 2 H), 1.85 (s, 4 H), 1.43 (s, 12 H), 0.96 (s, 18 H);  $^{13}\text{C NMR}$  (75 MHz,  $\text{CDCl}_3$ )  $\delta$  164.90, 77.45, 71.97, 70.92, 70.72, 70.42, 54.71, 54.66, 51.51, 41.43, 40.62, 31.86, 31.76, 30.34. MALDI-TOF-MS: calcd, 526.78  $[\text{M} + \text{H}]^+$ ; found, 526.44.

**G2 Surfactant.** Intermediate **3** (1.0 g, 1.0 mmol) is dissolved in 20 mL of chloroform, and DIPEA (0.2 mL, 1.5 mmol) is added to the solution. Jeffamine EDR-192 (1.0 g, 5.2 mmol) is added, and the solution is refluxed for 24 h. The crude product is concentrated and purified by silica gel chromatography using 9:1  $\text{CH}_2\text{Cl}_2/\text{CH}_3\text{OH}$  containing 1%  $\text{NH}_4\text{OH}$  as the eluent to give a white solid (0.68 g, 0.61 mmol) in 61% yield:  $^1\text{H NMR}$  (300 MHz,  $\text{CDCl}_3$ )  $\delta$  3.64 (m, 16 H), 3.40 (s, 24 H), 3.06 (s, 2 H), 2.73 (s, 2 H), 1.89 (s, 8 H), 1.66 (s, 8 H), 1.50 (s, 24 H), 1.00 (s, 36 H);  $^{13}\text{C NMR}$  (75 MHz,  $\text{CDCl}_3$ )  $\delta$  165.78, 164.52, 70.65, 70.21, 54.86, 54.81, 51.49, 40.82, 32.02, 31.92, 30.56. MALDI-TOF-MS: calcd, 1111.63  $[\text{M} + \text{H}]^+$ ; found, 1112.30.

**G2L Surfactant.** Intermediate **6** (1.5 g, 2.6 mmol) and intermediate **2** (1.2 g, 2.8 mmol) are dissolved in 50 mL of THF, and DIPEA (0.6 mL, 6.2 mmol) is added. After the solution is refluxed overnight, Jeffamine EDR-192 (2.5 g, 13 mmol) is added to the reaction mixture and allowed to react overnight at reflux. The solvent is evaporated, and the product is extracted with  $\text{CH}_2\text{Cl}_2$  and  $\text{H}_2\text{O}$ . After evaporation of the organic phase, the residue is purified by silica gel chromatography with 9:1  $\text{CHCl}_3/\text{CH}_3\text{OH}$  to give a white solid (1.7 g, 1.5 mmol) in 58% yield:  $^1\text{H NMR}$  (300 MHz,  $\text{CDCl}_3$ )  $\delta$  3.60 (bs, 12 H), 3.50 (bs, 4 H), 3.32 (bs, 8 H), 1.84 (s, 8 H), 1.56 (bs, 8 H), 1.40 (s, 24 H), 0.94 (s, 36 H);  $^{13}\text{C NMR}$  (75 MHz,  $\text{CDCl}_3$ )  $\delta$  165.68, 165.45, 165.20, 70.65, 70.40, 54.69, 54.56, 51.45, 40.78,



32.64, 31.86, 31.76, 30.40, 30.32, 27.80. ESI-MS: calcd, 1110.62 [M + H]<sup>+</sup>; found, 1110.90.

**G3 Surfactant.** Intermediate 5 (2.0 g, 0.94 mmol) is dissolved in 20 mL of chloroform, and DIPEA (0.2 mL, 1.5 mmol) is added to the solution. Jeffamine EDR-192 (1.0 g, 5.2 mmol) is added, and the solution is refluxed for 24 h. The crude product is concentrated and purified by silica gel chromatography using 9:1 CH<sub>2</sub>Cl<sub>2</sub>/CH<sub>3</sub>OH containing 1% NH<sub>4</sub>OH as the eluent to give a white solid (1.0 g, 0.44 mmol) in 47% yield: <sup>1</sup>H NMR (300 MHz, DMSO) δ 3.59 (t, 2 H), 3.48 (m, 12 H), 3.33 (s, 2 H), 3.16 (s, 24 H), 2.73 (s, 2 H), 1.83 (s, 16 H), 1.44 (s, 24 H), 1.36 (s, 48 H), 0.90 (s, 72 H); <sup>13</sup>C NMR (75 MHz, DMSO) δ 166.04, 165.40, 79.92, 70.48, 70.33, 54.10, 53.99, 50.74, 32.16, 32.08, 31.14, 27.95. MALDI-TOF-MS: calcd, 2281.32 [M + H]<sup>+</sup>; found, 2282.87.

**Intermediate 1.** Cyanuric chloride (20 g, 109 mmol) is dissolved in 200 mL of THF and cooled to 0 °C. *tert*-Octylamine (100 mL, 620 mmol) in THF is added dropwise over 30 min. The reaction is stirred for 24 h at 25 °C. The precipitate is removed by filtration. The filtrate is concentrated, and the resulting material is precipitated with cold methanol. The pure product is obtained in quantitative yields (40 g, 108 mmol): <sup>1</sup>H NMR (300 MHz, CDCl<sub>3</sub>) δ 1.84 (s, 4 H), 1.46 (s, 12 H), 0.98 (s, 18 H); <sup>13</sup>C NMR (75 MHz, CDCl<sub>3</sub>) δ 167.67, 164.64, 55.42, 51.40, 31.90, 31.72, 29.92, 29.64. ESI-MS: calcd, 370.27 [M + H]<sup>+</sup>; found, 370.27.

**Intermediate 2.** Intermediate 1 (30 g, 81 mmol) is dissolved in 500 mL of THF before DIPEA (15.0 mL, 86 mmol) and 1,4-butanediamine (24.6 mL, 21.4 g, 243 mmol) are added. The reaction is stirred for 24 h at reflux. The resulting material is purified by silica gel chromatography using 9:1 CH<sub>2</sub>Cl<sub>2</sub>/CH<sub>3</sub>OH to give a white solid (32 g, 76 mmol) in 94% yield: <sup>1</sup>H NMR (300 MHz, CDCl<sub>3</sub>) δ 3.30 (s, 2 H), 2.78 (t, 2 H), 2.67 (s, 2 H), 1.83 (s, 4 H), 1.56 (s, 4 H), 1.41 (s, 12 H), 0.96 (s, 18 H); <sup>13</sup>C NMR (75 MHz, CDCl<sub>3</sub>) δ 165.30, 54.63, 51.66, 41.82, 40.58, 31.84, 31.76, 30.33, 27.54. ESI-MS: calcd, 422.40 [M + H]<sup>+</sup>; found, 422.39.

**Intermediate 3.** Cyanuric chloride (1.2 g, 6.5 mmol) is dissolved in 50 mL of THF, and the solution is cooled to 0 °C before DIPEA (3.2 mL, 18 mmol) and intermediate 2 (5.5 g, 13 mmol) are added. After 30 min, the solution is allowed to warm to room temperature and stirred for an additional 6 h. Stirring is continued for another 18 h at 60 °C. The crude product is concentrated and purified by silica gel chromatography using 19:1 CH<sub>2</sub>Cl<sub>2</sub>/CH<sub>3</sub>OH. A white solid is obtained in quantitative yields (6.2 g, 6.5 mmol): <sup>1</sup>H NMR (300 MHz, CDCl<sub>3</sub>) δ 3.38 (s, 8 H), 1.86 (s, 8 H), 1.61 (s, 8 H), 1.43 (s, 24 H), 0.96 (s, 36 H); <sup>13</sup>C NMR (75 MHz, CDCl<sub>3</sub>) δ 165.68, 164.40, 54.91, 53.56, 51.40, 42.04, 40.58, 31.99, 31.87, 30.54. ESI-MS: calcd, 954.75 [M + H]<sup>+</sup>; found, 954.73.

**Intermediate 4.** Intermediate 3 (3.0 g, 3.1 mmol) is dissolved in 30 mL of THF before DIPEA (1.0 mL, 5.7 mmol) is added. Butanediamine (0.83 g, 9.4 mmol) is added, and the solution is heated to 100 °C for 24 h. The solvent is evaporated, and the material is purified by silica gel chromatography using 9:1 CH<sub>2</sub>Cl<sub>2</sub>/CH<sub>3</sub>OH to give a white solid (2.3 g, 2.3 mmol) in 74% yield: <sup>1</sup>H NMR (300 MHz, CDCl<sub>3</sub>) δ 3.32 (s, 10 H), 2.67 (t, 2 H), 1.83 (s, 8 H), 1.54 (s, 12 H), 1.40 (s, 24 H), 0.93 (s, 36 H); <sup>13</sup>C NMR (75 MHz, CDCl<sub>3</sub>) δ 166.27, 165.62, 165.36, 54.50, 51.55, 41.71, 40.95, 40.44, 31.81, 31.76, 30.40, 27.43. ESI-MS: calcd, 1006.87 [M + H]<sup>+</sup>; found, 1006.86.

**Intermediate 5.** Cyanuric chloride (0.10 g, 0.543 mmol) is dissolved in 10 mL of THF and cooled to 0 °C before DIPEA (0.5 mL, 2.9 mmol) and intermediate 4 (1.1 g, 1.1 mmol) are added. The reaction solution is allowed to warm to 25 °C with stirring for 6 h. Then, the reaction is continued for another 18 h at 100 °C. The crude product is concentrated and purified by silica gel chromatography using 19:1 CH<sub>2</sub>Cl<sub>2</sub>/CH<sub>3</sub>OH to give a white solid (0.79 g, 0.37 mmol) in 69% yield: <sup>1</sup>H NMR (300 MHz, CDCl<sub>3</sub>) δ 3.36 (m, 24 H), 1.87 (s, 16 H), 1.60 (m, 24 H), 1.44 (s, 48 H), 0.93 (s, 72 H); <sup>13</sup>C NMR (75 MHz, CDCl<sub>3</sub>) δ 166.04, 165.46, 164.56, 54.80, 53.59, 51.57, 41.45, 39.95, 39.32, 31.86, 31.77, 30.38. ESI-MS: calcd, 2123.70 [M + H]<sup>+</sup>; found, 2123.70.

**Intermediate 6.** Cyanuric chloride (2.0 g, 10.8 mmol) is dissolved in 100 mL of THF and cooled to 0 °C before DIPEA (4 mL, 23 mmol) and *tert*-octylamine (1.4 g, 10.8 mmol) are added. After stirring overnight at room temperature, 1,4-butanediamine (0.48 g, 5.4 mmol) is added. The reaction is refluxed overnight. The solvent is evaporated and the product recrystallized from hot methanol to give a white solid (2.0 g, 3.5 mmol) in 67% yield: <sup>1</sup>H NMR (300 MHz, CDCl<sub>3</sub>) δ 3.44 (bs, 4 H), 1.86 (s, 4 H), 1.67 (bs, 4 H), 1.44 (s, 12 H), 0.97 (s, 18 H); <sup>13</sup>C NMR (75 MHz, CDCl<sub>3</sub>) δ 167.88, 165.45, 164.71, 55.63, 51.17, 41.10, 31.83, 31.69, 29.64, 27.29. ESI-MS: calcd, 569.62 [M + H]<sup>+</sup>; found, 569.35.

**Sample Characterization.** The amount of organic material in each organoclay composite was determined using two independent methods. During the preparation of the composite, the amount of organic surfactant that was removed from the aqueous phase by the clay was measured (by subtraction) using UV-vis spectroscopy and a calibration curve. After washing and drying of the organoclay composite, the amount of organic material was measured using thermal gravimetric analysis (TGA). Both techniques were in excellent agreement (*vide infra*). The ILS was calculated by X-ray diffraction using a powder diffractometer [Bruker D8, 6°/min, Mo Kα source (0.71 Å)]. IR spectra (4021 Galaxy Series FT-IR) were recorded using KBr pellets after grinding of the sample.

## Results and Discussion

The discussion of the organoclays derived from these four surfactants is divided into seven sections. First, our nomenclature for these materials is introduced. Second, a comparison of the X-ray diffraction data derived from the **G1** surfactant, a molecule that behaves like a typical alkylammonium ion, is made with the data derived from the **G2** and **G3** surfactants that show that these dendritic surfactants do not appreciably change the ILS. In the third section, organoclays comprising **G2L** are introduced to dissect the role of size and shape. Fourth, the analysis of these materials by infrared spectroscopy is presented, which shows that interlayer water is retained for **G2** and **G3** materials but is absent in **G1** and **G2L** organoclays. This observation is corroborated by TGA analysis in the fifth section. Attempts to characterize these materials by transmission electron microscopy (TEM) are described in the sixth section. In the final section, we introduce a model to explain the intercalation behavior of the four surfactants.

**Surfactant-Dependent Relative Compositions.** The organoclay composites derived from the respective surfactants are named for the relative amount of organic material in the composite. Table 1 identifies these composites and shows the amount of surfactant as determined by both UV-vis spectroscopy and TGA. For example, when 100 mg of **G1** is mixed with 100 mg of clay, the resulting composite named **G1-50** appears to be of 48.0% and 49.8% organic content when analyzed

**Table 1. Percentage of Organic Material in Organoclay Composites from the G1 Surfactant from TGA and UV-Vis Analysis (Subtractive) of the Solution from Which the Composites Are Prepared**

name	TGA analysis (% organic)	UV-vis analysis (% organic)
<b>G1-5</b>	5.3	4.6
<b>G1-9</b>	9.2	9.0
<b>G1-17</b>	15.7	16.6
<b>G1-23</b>	20.2	22.6
<b>G1-29</b>	28.6	28.3
<b>G1-33</b>	31.2	32.7
<b>G1-50</b>	48.0	49.8

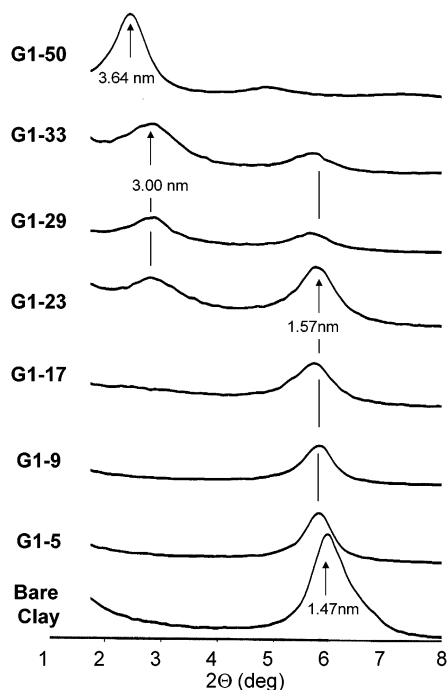


**Figure 1.** XPD of the **G1** organoclay composites.

by TGA and UV–vis spectroscopy, respectively. Similarly, **G1-23** comprises approximately 23% organic material. Attempts to prepare organoclay materials exceeding 50% organic material resulted in waxlike solids. The physical properties (i.e., aggregation, hydrophobicity) of these waxlike organoclays are noticeably different: these waxlike composites cannot be dried under reduced pressure or ground.

Unlike the smaller surfactant **G1**, the amount of organic materials in organoclays comprising **G2** and **G3** does not exceed that of **G2-12** and **G3-20**. In solutions containing higher concentrations of organic material, only **G2-12** and **G3-20** are obtained: the remaining organic material stays in solution and is removed upon filtration and/or washing. Interestingly, both concentrations of **G2** and **G3** correspond to approximately a 1:7 molar ratio of the surfactant to the number of the cationic sites present for exchange in the clay portion of the material. Conservation of  $6/7$  of the cationic sites in composites derived from larger, dendritic surfactants **G2** and **G3** is consistent with our assignment of a frustrated morphology. We hypothesize that these interior sites cannot be accessed because of the inability of these molecules to access the interlayer. On the contrary, **G1** forms organoclay materials at up to twice the cationic exchange capacity (CEC) of the clay.

**Evidence for Frustrated Intercalation from the ILS.** X-ray powder diffraction (XPD) confirms that, as **G1** is added to the clay, the ILS increases (Figure 1), as is expected in traditional small organic surfactants.<sup>2</sup> The ILS of the untreated calcium–smectite clay is 1.47 nm. Upon addition of **G1**, the ILS increases to 1.57 nm. At medium concentrations (23–33%) of **G1**, the ILS increases to 3.00 nm. This concentration of organic material corresponds to the CEC of the clay. At high concentrations (50%) of **G1**, the ILS shifts again to 3.64 nm.

In contrast to **G1** surfactants that appear to form a range of morphologies, the XPD traces of materials

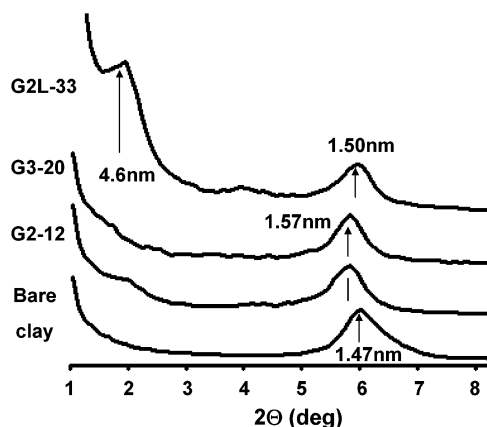


**Figure 2.** XPD of the **G2**, **G3**, and **G2L** organoclay composites.

derived from **G2** and **G3** show only a nominal increase in ILS to 1.57 nm, consistent with reduced loadings of these surfactants (Figure 2). It is unlikely that these large but conformationally flexible **G2** and **G3** molecules could penetrate the interlayer and remain in an extended, flat conformation, but this cannot be proven from XPD data. Instead, we favor frustrated intercalation wherein these molecules are confined to the surface of these materials.

**The Role of Shape.** To better evaluate the role of shape in these composites, a linear isomer of **G2**, **G2L**, was prepared and evaluated. As with **G1**, **G2L** shows a linear correlation between the amount of surfactant added (5–33%) to a solution of clay and the amount of surfactant incorporated as determined by TGA. These values differ greatly from the dendritic molecule **G2**: organoclays are limited to 12% organic content. XPD traces are consistent with the appearance of a new morphology at high loadings of **G2L** when the organic content exceeds 17% (w/w). While the predominant morphology appears to be monolayer adsorption showing an ILS of 1.5 nm over the entire range, at higher loadings of surfactant, an intermediate ILS of 2.3 nm and a final (but poorly resolved because of limitations of the instrument) ILS of 4.6–5.2 nm are observed for **G2L-33**. This distance corresponds to the fully extended dimensions of the linear surfactant calculated to be  $\sim 3.6$  nm.

**Evidence for Frustrated Intercalation from Interlayer Water: IR Spectroscopy.** At ambient temperature and humidity, water is present in the interlayer of the clays. Bare clay shows two characteristic water bands (Figure 3): tightly bound interlayer water appears at  $\sim 1635$   $\text{cm}^{-1}$  in the bare clay, and a broader O–H absorption band appears around  $3300$   $\text{cm}^{-1}$ .<sup>1</sup> Water loss can occur when cationic surfactants displace the exchangeable inorganic cations and their associated water molecules. The surfactant shows two characteristic aromatic stretches at  $1514$  and  $1574$   $\text{cm}^{-1}$  as well as in the aliphatic C–H region at  $\sim 2950$   $\text{cm}^{-1}$ . These stretches appear in the organoclays as well. IR features at both  $1635$  and  $3300$   $\text{cm}^{-1}$  are notably reduced in **G1-33** and **G2L-33** as the organic molecules displace molecules of water from the interlayer. For molecules displaying frustrated intercalation, the interlayer water should be preserved. Indeed, the stretch for tightly bound water at  $1635$   $\text{cm}^{-1}$  for **G2-12** appears to be more

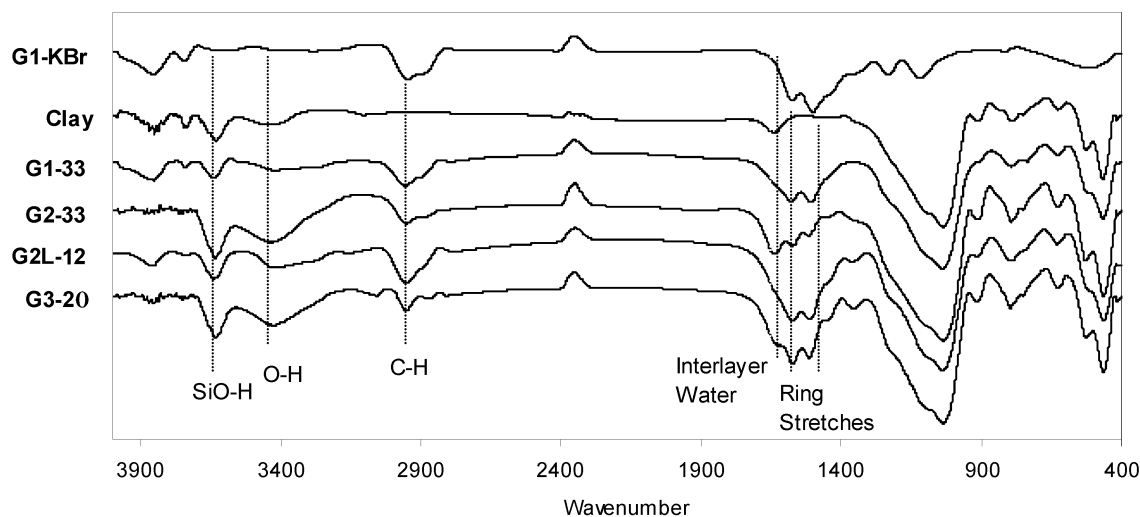


**Figure 3.** IR spectra of **G1**, clay, **G1-33**, **G2-33**, **G2L-12**, and **G3-20**.

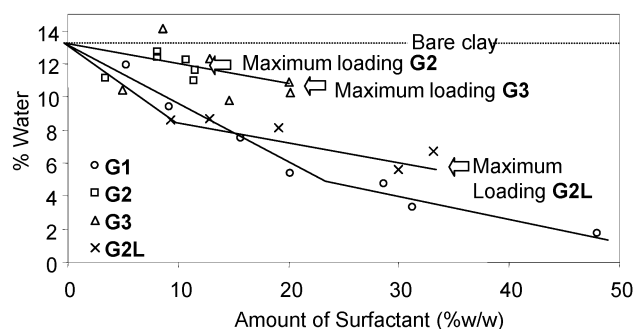


**Figure 4.** Water content as a function of relative composition. Both **G1** and **G2L** show significant dehydration as the amount of organic is increased. This loss of interlayer water is not as evident in **G2** and **G3**. The dashed line corresponds to bare clay. The solid lines are intended to guide the eye and do not represent a fit of the data.

dominant than the aromatic stretches. This band also appears as a significant shoulder for **G3-20**.

**Evidence for Frustrated Intercalation from Interlayer Water: TGA.** TGA confirms the data from IR spectroscopy. Across the entire range of organoclay morphologies derived from **G1**, TGA reveals that, as the amount of **G1** surfactant is increased, the amount of water present in the interlayer (as revealed by the thermal transitions below 150 °C) is greatly reduced (Figure 4). A similar trend is observed for **G2L**. On the contrary, molecules showing frustrated intercalation do not show appreciable water loss.

**Microscopy Is Inconclusive.** We attempted to characterize the ILS that resulted from the addition of **G1** surfactant by TEM, but such investigations proved unsatisfying beyond establishing the integrity of the composite. Fringes were observed in these samples, suggesting that the clay retains its flexibility, but these fringes did not provide a spacing that was consistent with the XPD data (3.6 nm): the TEM image from **G1-33** shows fringes ranging from 1 to 2 nm. We cannot distinguish between heterogeneity in the sample or localized destruction of the morphology during the course of the experiment. TGA reveals that the surfactant is lost sharply over a temperature range of 175–200 °C, values consistent with estimations of the local temperature due to electron bombardment.

**Our Conceptual Model.** Based on the data from XPD, TGA, and IR and the dimensions of the surfactants, our conceptual model for intercalation is shown in Scheme 3. As increasing amounts of **G1** are added, the clay interlayer separates to form three different morphologies: (i) surfactant lying flat on the surface of the clay or extending from the interlayer; (ii) a semi-ordered mono- or bilayer in which the hydrophobic groups aggregate away from the hydrophilic clay surface; (iii) a more order layered structure resulting from a fully extended surfactant. The surfactant is approximately 2.4 nm when fully extended. These values are consistent with those of the proposed model. For **G2** and **G3**, however, the predominant morphology, frustrated intercalation, is shown in part iv with the dendritic portion extending into the solvent. A model similar to **G1** can be applied to **G2L** (v). These models are now the focus of computational investigations that will be reported in due course.

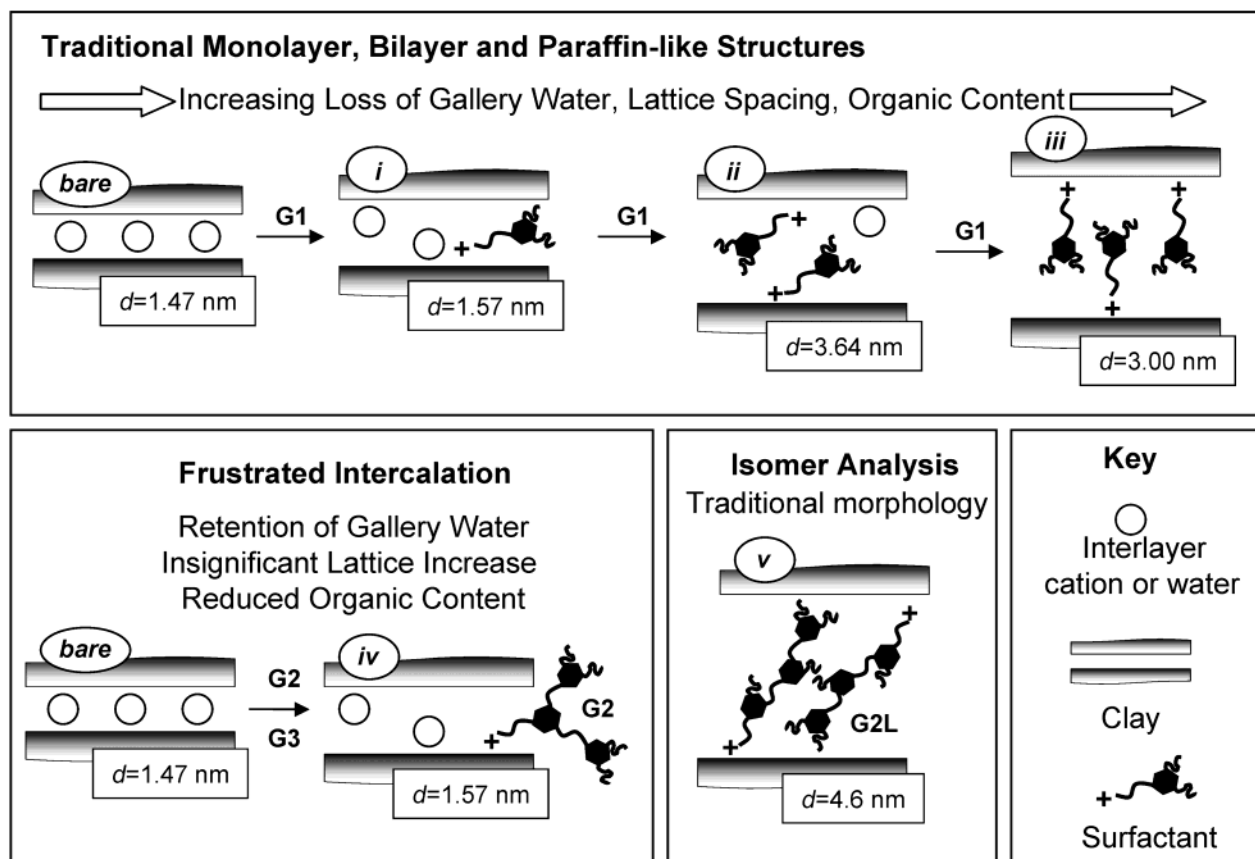
## Conclusions

The organoclay architectures reported here are notably different than the traditional monolayer, bilayer, and paraffinlike structures first described beginning more than 50 years ago.<sup>1</sup> The data presented here—small lattice spacings, a hydrophilic gallery, linear versus branched isomer comparison—is consistent for a new morphology of organoclay composites in which a large branching group attached to a linear anchor precludes complete intercalation of the organic component into the interlayer gallery. We describe this morphology as “frustrated intercalation”.

Interestingly, a morphology similar to this one has been hypothesized in a linear polycation wherein complete penetration is precluded enthalpically. As the polycation reptates into the interlayer, increasing numbers of clay–polycation interactions increasingly retard penetration to the limit where much of the polycation remains accumulated at the surface, with portions of the molecule freely interacting with solution. In these systems surface coverage rarely exceeds 50%.<sup>3,20</sup> Frustrated

(20) Lagaly, G. In *Proceedings of the International Clay Conference*, Denver, CO, 1985; Shultz, L. G., an Olphen, H., Mumpton, F. A., Eds.; Clay Mineral Society: Bloomington, MN, 1985; pp 232–251.



Scheme 3. Morphological Model Useful for Rationalizing XPD Data<sup>a</sup>

<sup>a</sup> As the amount of **G1** increases, different morphologies with characteristic ILS are observed (i–iii). **G2** (shown) and **G3** yield a single morphology, frustrated intercalation (iv), while **G2L** shows a structure similar to that of **G1** (v).

trated intercalation may produce similar effects but by a different mechanism. In frustrated intercalation, failure to completely intercalate in this gallery is the result of shape and not the result of multivalent anchoring of the surfactant to the clay surface. The role of sterics and shape in these architectures is further supported by the preparation and examination of the linear analogue **G2L**, a molecule that enters the interlayer, increases lattice spacing, and decreases the amount of bound water. In both morphologies, the organic component remains on the surface of the clay particle.

Definitively establishing morphologies for organoclay composites not only is challenging but relies on the accumulation of inference from a variety of systems.

Additional studies will be required to evaluate whether this type of morphology is general and whether our conceptual model is accurate. Computational and experimental studies are currently underway. We find these architectures intriguing: they should allow for the surface of a clay particle to be selectively tailored without sacrificing surfactant to the interlayer.

**Acknowledgment.** This work was supported by the Welch Foundation (A-1430) and the USDA-CSREES 2002-35102-12504.

CM0302328